THE JOURNAL OF BIOLOGICAL CHEMISTRY VOL. 290, NO. 25, pp. 15892–15903, June 19, 2015

The Function of Embryonic Stem Cell-expressed RAS (E-RAS), a Unique RAS Family Member, Correlates with Its Additional Motifs and Its Structural Properties*[S]

Received for publication, January 28, 2015, and in revised form, April 21, 2015 Published, JBC Papers in Press, May 4, 2015, DOI 10.1074/jbc.M115.640607

Saeideh Nakhaei-Rad[‡], Hossein Nakhaeizadeh[‡], Claus Kordes[§], Ion C. Cirstea[‡¶], Malte Schmick[‖], Radovan Dvorsky[‡], Philippe I. H. Bastiaens[‖], Dieter Häussinger[§], and Mohammad Reza Ahmadian[‡1]

From the [‡]Institute of Biochemistry and Molecular Biology II and [§]Clinic of Gastroenterology, Hepatology, and Infectious Diseases, Medical Faculty of the Heinrich-Heine University, 40255 Düsseldorf, the [¶]Leibniz Institute for Age Research-Fritz Lipmann Institute, 07745 Jena, and the [‖]Department of Systemic Cell Biology, Max Planck Institute of Molecular Physiology, 44227 Dortmund, Germany

Background: E-RAS contains additional motifs and regions with unknown functions.
Results: Biochemical analysis reveals that effector selection of E-RAS significantly differs from H-RAS.
Conclusion: E-RAS selectivity and consequently cellular outcomes depend on its unique switch and interswitch regions.
Significance: E-RAS possesses specific sequence fingerprints and therefore no overlapping function with H-RAS.

E-RAS is a member of the RAS family specifically expressed in embryonic stem cells, gastric tumors, and hepatic stellate cells. Unlike classical RAS isoforms (H-, N-, and K-RAS4B), E-RAS has, in addition to striking and remarkable sequence deviations, an extended 38-amino acid-long unique N-terminal region with still unknown functions. We investigated the molecular mechanism of E-RAS regulation and function with respect to its sequence and structural features. We found that N-terminal extension of E-RAS is important for E-RAS signaling activity. E-RAS protein most remarkably revealed a different mode of effector interaction as compared with H-RAS, which correlates with deviations in the effector-binding site of E-RAS. Of all these residues, tryptophan 79 (arginine 41 in H-RAS), in the interswitch region, modulates the effector selectivity of RAS proteins from H-RAS to E-RAS features.

Small GTPases of the RAS family act as molecular switches within the cell, cycling between a GTP-bound (active) and a GDP-bound (inactive) state (1, 2). These molecules trigger intracellular responses by sensing the extracellular signals through their interacting receptors or intermediate proteins and passing the signal to downstream targets. Therefore, they play a key role in various cellular processes, including gene expression, metabolism, cell cycle progression, proliferation, survival, and differentiation. Somatic or germ line mutations in genes related to members of the RAS family or their regulators are commonly associated with cancer progression or developmental disorders (3–9).

The best investigated RAS proteins are H-, N-, and K-RAS4B, which share overlapping functions, including cell proliferation, differentiation, and apoptosis (10–13). However, different RAS isoforms exhibit a particular pattern of expression, different regulators, and specific microdomains or subcellular localization, indicating their functional specificity as well as redundant roles (10–17). The individual roles of other members of the RAS family, such as R-RAS, TC21, M-RAS, AGS-1, or the embryonic stem cell-expressed RAS (E-RAS), have not been fully described. E-RAS was identified in 2003 as a new member of the RAS family, which is specifically expressed in undifferentiated mouse embryonic stem cells (18). In addition to stem cells, E-RAS has been detected in the several adult cynomolgus tissues (19) and in gastric cancer and neuroblastoma cell lines (20, 21).

Plasma membrane localization of the classical RAS isoforms (H-, N-, and K-RAS4B) has been shown to be critical for their functionality (22–24). The membrane association is achieved by post-translational modifications (PTMs)[2] at the C terminus of RAS proteins. H-RAS and N-RAS undergo two types of PTMs, farnesylation at a cysteine residue in C*AAX* (where C is cysteine, *A* is any aliphatic amino acid, and *X* is any amino acid) motifs and palmitoylation of one or two cysteine residues in the hypervariable region (HVR) (23, 25–27). K-RAS4B lacks the cysteine residues in its HVR; instead it has a basic sequence of six lysines that maintains its strong association with the plasma membrane (24, 28, 29).

RAS proteins are inefficient GTP-hydrolyzing enzymes. Such an intrinsic GTPase reaction requires stimulation through GTPase-activating proteins (GAPs) by orders of magnitude (30–32). However, GDP dissociation is also a very slow

* This work was supported in part by the German Research Foundation through Collaborative Research Center 974 (Grant SFB 974), Communication and Systems Relevance during Liver Injury and Regeneration. The authors declare that they have no conflicts of interest with the contents of this article.
[S] This article contains supplemental Fig. S1.
[1] To whom correspondence should be addressed: Institut für Biochemie und Molekularbiologie II, Medizinische Fakultät der Heinrich-Heine-Universität, Universitätsstr. 1, Gebäude 22.03.03, 40255 Düsseldorf, Germany. Tel.: 49-211-81-12384; Fax: 49-211-81-12726; E-mail: reza.ahmadian@uni-duesseldorf.de.

[2] The abbreviations used are: PTM, post-translational modification; RBD, RAS-binding domain; aa, amino acid; GEF, guanine nucleotide exchange factor; PLC, phospholipase C; PDB, Protein Data Bank; MDCK, Madin-Darby canine kidney cell; HVR, hypervariable region; PIP_3, phosphoinositide 3,4,5-trisphosphate; RA, RAS association; GAP, GTPase-activating protein; EYFP, enhanced YFP.

reaction that needs acceleration by guanine nucleotide exchange factors (GEFs) (33, 34). RAS proteins share a highly conserved GTP-binding (G) domain with five essential motifs, termed G1 to G5 (supplemental Fig. S1) (35, 36). G1 or the P-loop (^{10}G*XXXX*GK(S/T)^{17}; H-RAS numbering) binds the β- and γ-phosphates of GTP (37). Substitution of glycine 12 to any other amino acid (except for proline) is most frequently found in human cancers. These mutations render RAS protein GAP-insensitive and consequently hyperactive (7, 38). G2 and G3, also referred to as switch I and switch II, respectively, are dynamic regions that sense the nucleotide state and provide the regulator and effector-binding sites (1, 39). G4 and G5 are important for determining the guanine base-binding specificity of the G domain (40, 41). Sequence analysis revealed that E-RAS contains a G domain with five fingerprint sequence motifs almost identical to classical RAS proteins indicating that it is a functional GTP-binding protein (supplemental Fig. S1). However, E-RAS contains a serine instead of glycine 12 (H-RAS numbering), making it GAP-insensitive (18).

H-, N-, and K-RAS4B share an identical effector binding regions (switch I and II; supplemental Fig. S1), suggesting that they may share the same downstream effectors. In contrast, E-RAS revealed significant differences in the effector binding regions (supplemental Fig. S1). This implicates that it may utilize other effectors as compared with known H-RAS effectors and may consequently have different cellular functions. However, the downstream effectors selective for E-RAS are not fully identified yet. A known H-RAS effector is phosphoinositide 3-kinase (PI3K) that has also been reported to be activated by E-RAS (18, 27, 42).

In addition to effector binding regions, E-RAS is distinguished from the classical RAS isoforms due to its unique extended N terminus (Fig. 1*A* and supplemental Fig. S1). This may provide a putative interaction site for a new group of proteins, which may determine its subcellular localization. For instance, it contains a P*XX*P motif that may serve as a putative binding motif for interaction with Src homology 3-containing proteins. In this study, we comprehensively investigated human E-RAS and its variants regarding their cellular localization and functional and structural properties in direct comparison with H-RAS wild-type and its G12V hyperactive variant. We found that N-terminal extension of E-RAS is important for E-RAS signaling activity. E-RAS protein most remarkably revealed different effector selectivity as compared with H-RAS, which is influenced by deviations in the effector-binding site of E-RAS. Data presented in this study implicate that in addition to switch regions, the interswitch region of E-RAS also contributes to high affinity binding to PI3Kα and low affinity to other RAS effectors, including RASSF5/Nore1, RAF1, Ral guanine nucleotide dissociation stimulator (RalGDS), and phospholipase Cϵ (PLCϵ).

Materials and Methods

Constructs—Human *E-RAS* cDNA was obtained from pCMV6-AC-hsE-RAS (Origene). Human *H-RAS* was obtained from ptacH-RAS (43). $H\text{-}RAS^{Val\text{-}12}$, $E\text{-}RAS^{Ser\text{-}226/Ser\text{-}228}$, $E\text{-}RAS^{Ser\text{-}7}$, and $E\text{-}RAS^{Ala\text{-}31/Ala\text{-}32/Ala\text{-}33}$ were generated by PCR-based site-directed mutagenesis as described (32). The E-RAS with the N-terminal deletion, lacking the first 38 amino acids (aa) ($E\text{-}RAS^{\Delta N}$), was designed using primers to amplify *E-RAS* cDNA starting from aa 39 and ending with aa 233 (supplemental Fig. S1). The same primers were used to generate $E\text{-}RAS^{\Delta N/Ser\text{-}226/Ser\text{-}228}$ (palmitoylation-dead variant of *E-RAS* lacking the N terminus) using $E\text{-}RAS^{Ser\text{-}226/Ser\text{-}228}$ as template. To generate E-RAS constructs with mutations in their effector binding regions, we used $E\text{-}RAS^{WT}$ cDNA as template. First, $E\text{-}RAS^{SwI}$ (H70Y/Q75E; Tyr-32 and Glu-37 in H-RAS), $E\text{-}RAS^{Arg\text{-}79}$ (W79R; Arg-41 in H-RAS), and $E\text{-}RAS^{SwII}$ (A100E/I101E/H102Y/R103S; Glu-62, Glu-63, Tyr-64, and Ser-65 in H-RAS) were generated. These constructs were used to generate $E\text{-}RAS^{SwI/Arg\text{-}79}$, $E\text{-}RAS^{SwI/SwII}$, $E\text{-}RAS^{Arg\text{-}79/SwII}$, and $E\text{-}RAS^{SwI/Arg\text{-}79/SwII}$, respectively. All cDNAs were amplified via PCR and subcloned via BamHI/XhoI in pcDNA 3.1 vector with an N-terminal FLAG tag or EcoRI/BamHI in pEYFP-C1.

Cell Culture and Transfection—MDCK II and COS-7 cells were cultured in Dulbecco's modified Eagle's medium (DMEM) supplemented with 10% fetal calf serum (FCS) and 50 units of penicillin/streptomycin (Gibco® Life Technologies, Inc.). Transfection was performed by using TurboFect transfection reagent, according to manufacturer's protocol (Life Technologies, Inc.).

Immunostaining—Cells were fixed with 4% paraformaldehyde for 20 min at room temperature. After washing with PBS, the cells were permeabilized with 0.25% Triton X-100/PBS for 5 min and washed again. For blocking, the cells were treated 1 h with PBS containing 0.25% Triton X-100 and 3% bovine serum albumin (BSA, Merck) at room temperature, then incubated with primary antibodies for 1 h, then washed three times, followed by incubation with secondary antibodies for 2 h at room temperature. The coverslips were mounted using ProLong® Gold antifade reagent contained DAPI dye (Life Technologies, Inc.). Primary antibodies were rabbit anti-FLAG (1:700, catalog no. F7425 Sigma) and mouse anti-Na^+/K^+-ATPase (1:100, catalog no. A275 Sigma), and secondary antibodies Alexa 488-conjugated goat anti-rabbit IgG (1:500, catalog no. A11008, Life Technologies, Inc.) and Alexa 546-conjugated goat anti-mouse IgG (1:500, catalog no. A11003, Life Technologies, Inc.). The images were taken by using an LSM 510-Meta microscope (Zeiss) at excitation wavelengths of 364, 488, and 546 nm.

Live Cell Imaging—MDCK II cells were seeded on Permanox 8-well chambered slides (Lab-Tek, Nunc). LSM 510-Meta microscope (Zeiss) was equipped with ×63 immersion objective, and fluorescent fusion proteins were excited using lasers with 504 nm (YFP) wavelength. An environmental chamber holds the temperature at 37 °C, and the cells were maintained in imaging medium.

Pulldown Assay and Immunoblotting—The RAS-binding domain (RBD) of RAF1 (aa 51–131), the RAS association (RA) domain of RalGDS (aa 777–872), the RA domain of PLCϵ (aa 2130–2240), the RBD of p110α (aa 127–314), the catalytic subunit of PI3Kα, and the RA domain of RASSF5 (aa 200–358) were inserted in pGEX-4T vector and expressed in *Escherichia coli* to obtain GST-fused proteins. Bacterial lysates were used to pulldown GTP-bound RAS proteins from total cell lysates. GST pulldown and immunoblotting using rabbit anti-FLAG (1:5000, catalog no. F7425 Sigma) and rat anti-α-tubulin (1:2000, SM 568, Acris) were carried out as described previously (44). In

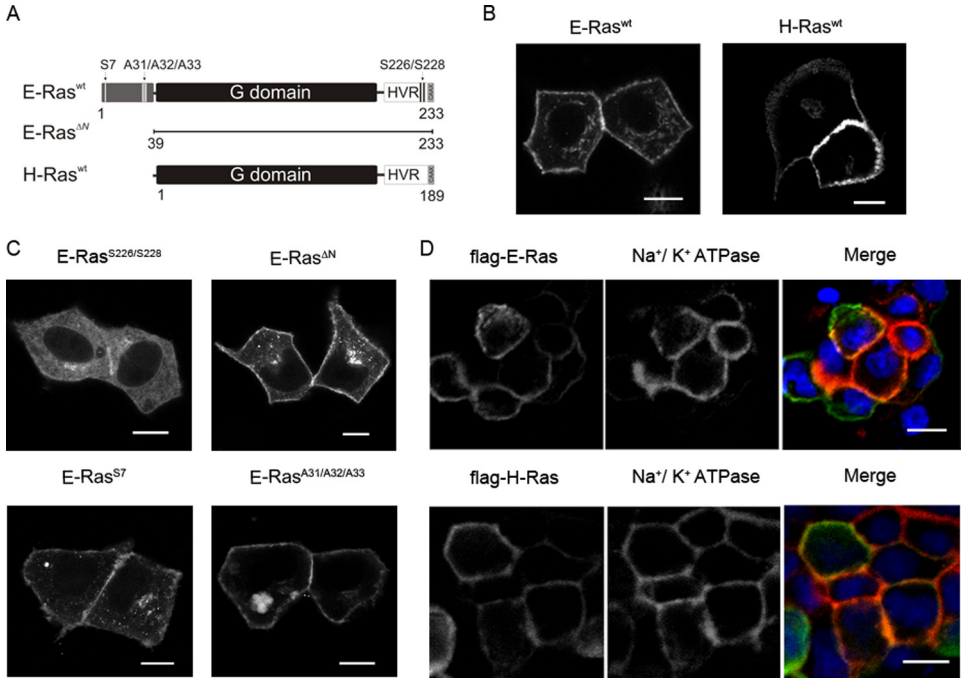

FIGURE 1. **Human E-RAS is largely associated with plasma membrane and some regions of E-RAS modulating its cellular localization.** *A*, different E-RAS variants used in this study, including N-terminal truncated E-RAS$^{\Delta N}$ (aa 39–233), palmitoylation-deficient E-RAS$^{Ser\text{-}226/Ser\text{-}228}$ (aa 1–233), N-terminal putative P*XX*P motif mutant E-RAS$^{Ser\text{-}7}$ (aa 1–233), and an N-terminal triple arginine motif variant E-RAS$^{Ala\text{-}31/Ala\text{-}32/Ala\text{-}33}$ (aa 1–233). *B* and *C*, confocal live images of transiently transfected MDCK II cells with EYFP-tagged E-RAS^{WT}, H-RAS^{WT}, E-RAS$^{Ser\text{-}226/Ser\text{-}228}$, E-RAS$^{\Delta N}$, E-RAS$^{Ser\text{-}7}$, and E-RAS$^{Ala\text{-}31/Ala\text{-}32/Ala\text{-}33}$. *D*, confocal imaging was performed using transiently transfected MDCK II cells with E-RAS and H-RAS. FLAG-tagged E-RAS co-localized with Na^+/K^+-ATPase to the plasma membrane, very similar to H-RAS, which was used as a control. *Scale bar,* 10 μm.

parallel, the cell lysates were used to visualize phospho-MEK1/2, phospho-ERK1/2, and phospho-AKT proteins states, respectively, using antibodies against MEK1/2 (Cell Signaling^{TM}), ERK1/2 (Cell Signaling^{TM}), AKT (Cell Signaling^{TM}), phospho-MEK1/2 (Ser-217/S221, Cell Signaling^{TM}), phospho-ERK1/2 (Thr-202/Thr-204, Cell Signaling^{TM}), and phospho-AKT (Ser-473 and Thr-308, Cell Signaling) in immunoblotting. All antibodies were diluted in 5% nonfat milk (Carl Roth GmbH).

Structural Methods—The structures of H-RAS were used in our study because no E-RAS structure was available to date. The G domains of H-RAS and E-RAS share 48% identity and were originally described to be structurally very similar, if not identical (18). The interactions with potential binding partners were analyzed on the basis of the structures of H-RAS in complexes with p120RASGAP (PDB code 1WQ1) (30), the RASGEF SOS1 (PDB codes 1NVV (45) and 4NYI), and the downstream effectors RAF1-RBD (PDB codes 1C1Y and 3KUD) (46, 47), PI3Kγ (PDB code 1HE8) (48), BYR2-RBD (PDB code 1K8R) (49), RalGDS (PDB code 1LFD) (50), PLC1 (PDB code 2C5L) (51), Grb14 (PDB code 4K81) (52), and RASSF5 (PDB code 3DDCS) (53).

Results

N Terminus Is an Important Factor for E-RAS Function—The cellular localizations of FLAG-tagged and EYFP-tagged wild-type E-RAS (E-RAS^{WT}) were investigated in direct comparison with H-RAS^{WT} in MDCK II cells. Confocal imaging revealed that E-RAS, very similar to H-RAS, is mainly associated with the plasma membrane (Fig. 1*B*) as it is co-localized with the basolateral membrane marker of sodium/potassium-ATPase (Fig. 1*D*). This result clearly suggests that E-RAS undergoes post-translational modifications, *e.g.* farnesylation and palmitoylation, at the very C-terminal cysteines (supplemental Fig. S1). Accordingly, a palmitoylation-deficient E-RAS$^{Ser\text{-}226/Ser\text{-}228}$ variant clearly exhibited a cytoplasmic accumulation, which supports the notion that E-RAS also underlies a palmitoylation/depalmitoylation mechanism as was shown previously for H-RAS (Fig. 1*C*) (25).

Another question addressed in this study was the role of the 38-amino acid unique N-terminal extension in E-RAS, which does not exist in other RAS proteins (Supplemental Fig. S1). This extension contains motifs, which may act either as a P*XX*P motif-binding site for specific Src homology 3-containing proteins or as an electrostatic interaction site (RRR motif) with a negatively charged region of proteins or with a lipid membrane. Thus, one function of the N-terminal extension and its motifs could be providing an additional signal for subcellular localization of E-RAS. Hence, we generated the N-terminal truncated E-RAS$^{\Delta N}$ (aa 39–233), putative P*XX*P motif variant E-RAS$^{Ser\text{-}7}$ (aa 1–233), and a triple arginine motif variant E-RAS$^{Ala\text{-}31/Ala\text{-}32/Ala\text{-}33}$ (aa 1–233) (Fig. 1*A*), and we investigated their localization in transiently transfected MDCK II cells. Confocal imaging of the EYFP-fused E-RAS variants revealed that the N terminus of E-RAS has a slight effect on the E-RAS localization as we observed for the truncated N-terminal variant E-RAS$^{\Delta N}$, putative P*XX*P motif variant E-RAS$^{Ser\text{-}7}$, and E-RAS$^{Ala\text{-}31/Ala\text{-}32/Ala\text{-}33}$-less plasma membrane localization (Fig. 1*C*) but not significant differences.

Effector Selection of E-RAS Significantly Differs from H-RAS—Before investigating the specific function of E-RAS in cells, it was important to gain insights into the E-RAS effector selectiv-

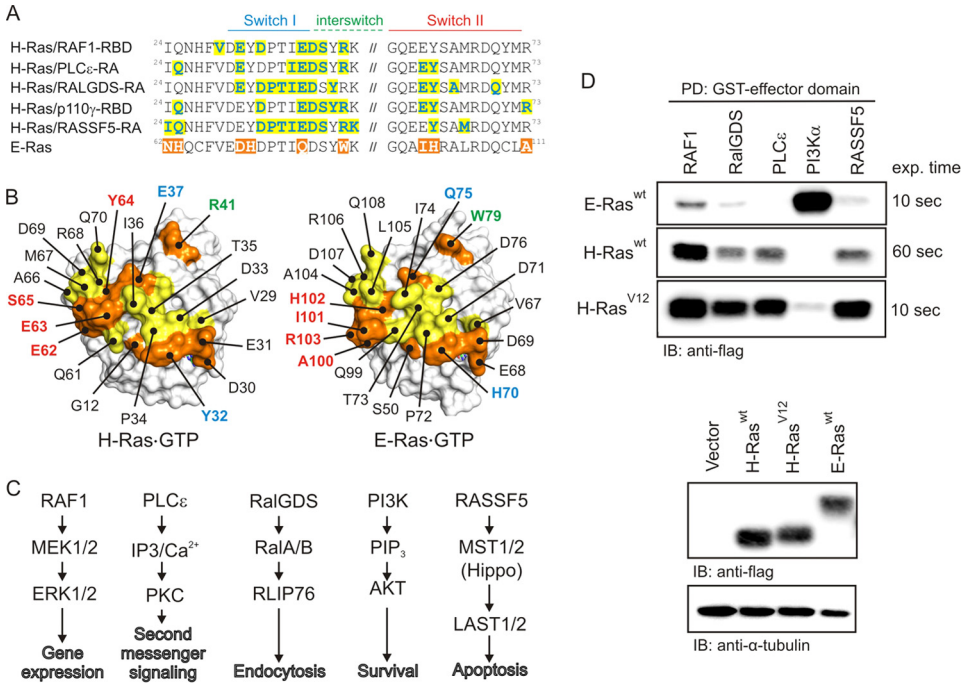

FIGURE 2. **Different effector selection of E-RAS and H-RAS.** *A,* effector-binding residues of H-RAS, obtained from various crystal structures, are highlighted with *blue letters* and *yellow background*, RAF1 (PDB code 1C1Y), PLCϵ (PDB code 2C5L), RalGDS (PDB code 1LFD), PI3Kγ (PDB code 1HE8), and RASSF5 (PDB code 3DDC). *B,* effector binding regions (in *yellow* and *orange*) of H-RAS and E-RAS were structurally analyzed on the basis of the H-RAS structure in complexes with p120RASGAP (PDB code 1WQ1). The *orange* amino acids indicate the sequence deviation between H-RAS and E-RAS. *C,* schematic view of RAS effector pathways and their cellular functions. *D,* E-RAS and H-RAS pulldown (*PD*) with various RAS effectors using COS-7 cell lysates transiently transfected with FLAG-tagged E-RAS^{WT}, H-RAS^{WT}, and H-RAS^{Val-12} using GST-fused effector proteins, such as RAF1-RBD, RalGDS-RA, PLCϵ-RA, PI3Kα-RBD, and RASSF5-RA. RAS proteins were analysis by immunoblot using an anti-FLAG antibody. Immunoblots (*IB*) of total cell lysates were used as a control to detect FLAG-RAS. *Exp. time* stands for exposure time. *RAF,* rapidly accelerated fibrosarcoma; *MEK,* mitogen-activated protein kinase/ERK kinase; *ERK,* extracellular signal-regulated kinase; *PLCϵ,* phospholipase Cϵ; *PKC,* protein kinase C; *RalGDS,* Ral GDP dissociation stimulator; *RLIP76,* Ral-interacting protein 76 kDa; *PI3K,* phosphoinositide 3-kinase; *PIP_3,* phosphoinositide 3,4,5-trisphosphate; *MST1/2,* mammalian Ste20-like kinases 1.

ity. Effector interactions with H-RAS have been investigated both biochemically and structurally in great detail. Various amino acids of H-RAS undergo selective contacts with the effectors, including RAF1, RalGDS, RASSF5, and PLCϵ (Fig. 2*A*, *blue residues* with *yellow background*). These residues, mainly switch I, interswitch, and partially in the switch II region, are conserved among common RAS proteins but vary in E-RAS proteins (supplemental Fig. S1). This suggests that classical RAS family members, except the E-RAS, are in principle able to recognize and activate various effectors. Importantly, these effector-binding residues are highly variable between H-RAS and E-RAS (supplemental Fig. S1; Fig. 2*A*). Structural analysis of the effector binding regions of E-RAS was performed according to H-RAS complexes with p120RASGAP (PDB code 1WQ1). In comparison with H-RAS, the exposed residues along the effector-binding surface of E-RAS revealed significant sequence deviations (Fig. 2*B*). This strongly indicates a differential effector selectivity of the RAS proteins.

The members of the RAS family are known to interact with a wide range of effectors (5, 54–61) and therefore stimulate various cellular responses. Regarding their physical interaction with E-RAS and H-RAS proteins, five RAS effectors (RAF1, RalGDS, PLCϵ, PI3Kα, and RASSF5), with defined cellular functions (Fig. 2*C*), were investigated in this study. In pulldown experiments, GST-fused RAS-binding domain of RAF1 (RAF1-RBD), the RAS association domain of RalGDS (RalGDS-RA), PLCϵ-RA, PI3Kα-RBD, and RASSF5-RA were used as baits to pulldown FLAG-tagged E-RAS^{WT}, H-RAS^{WT}, and H-RAS^{Val-12} overexpressed in COS-7 cells. We found that H-RAS^{WT} and H-RAS^{Val-12} strongly bind RAF1 and weakly bind to PI3Kα. Importantly, E-RAS^{WT} clearly showed an opposite pattern of these interactions, where it binds very tightly to PI3Kα and very weakly to RAF1, RalGDS, PLCϵ, and RASSF5 (Fig. 2*D*). These data confirm that the amino acid deviations in effector-binding sites (Fig. 2, *A* and *B*) make E-RAS a unique member of the RAS family and a potent activator of the PI3K-PIP_3-signaling pathways.

Effector Selection by E-RAS Is Largely Determined by Tryptophan 79—To identify the residues determining the specificity for effector binding and activation, we next analyzed the impact of deviating residues in E-RAS on its interaction with different effectors by replacing the E-RAS residues in switch I (His-70 and Gln-75, collectively named here SwI), interswitch (Arg-79), and switch II (Ala-100, Ile-101, His-102, and Arg-103, collectively named here SwII) for the equivalent residues in H-RAS (supplemental Fig. S1). The corresponding variants, E-RAS^{SwI}, E-RAS^{Arg-79}, E-RAS^{SwII}, E-RAS$^{SwI/Arg-79}$, E-RAS$^{Arg-79/SwII}$, RAS$^{SwI/SwII}$, and E-RAS$^{SwI/Arg-79/SwII}$ (Fig. 3*A*), were analyzed for their interaction abilities with different effectors using E-RAS^{WT} and the constitutive active variant of H-RAS^{wt}, H-RAS^{Val-12}, as controls. These constructs were transiently transfected in COS-7 cells, and the GTP-bound forms of these RAS variants were pulled down using GST-fused effector proteins under the same conditions as described above. Data

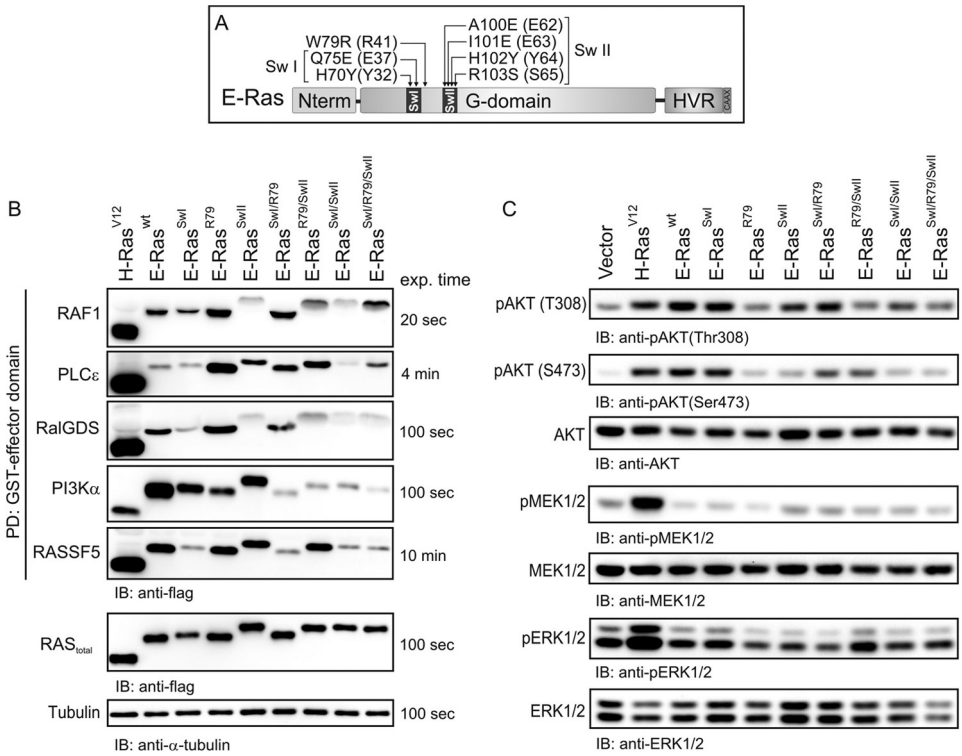

FIGURE 3. **Specificity-determining residues in E-RAS-effector interaction.** *A*, display of different effector binding mutations in E-RAS: E-RAS^{SwI}, H70Y/Q75E (Tyr-32 and Gslu-37 in H-RAS); E-RAS^{Arg-79}, W79R (Arg-41 in H-RAS); E-RAS^{SwII}, A100E/I101E/H102Y/R103S (Glu-62, Glu-63, Tyr-64, and Ser-65 in H-RAS); E-RAS$^{SwI/Arg-79}$, H70Y/Q75E/W79R; E-RAS$^{Arg-79/SwII}$, W79R/A100E/I101E/H102Y/R103S; RAS$^{SwI/SwII}$, H70Y/Q75E/A100E/I101E/H102Y/R103S, and E-RAS$^{SwI/Arg-79/SwII}$, H70Y/Q75E/W79R/A100E/I101E/H102Y/R103S. For details about the amino acid sequences, see supplemental Fig. S1. *B,* pulldown assay of FLAG-fused E-RAS variants carried out with RBD or RA domain of GST-fused effector proteins, including RAF1-RBD, RalGDS-RA, PLCε-RA, PI3Kα-RBD, and RASSF5-RA. The results were analyzed by immunoblot using an anti-FLAG antibody. *Exp. time* stands for exposure time. *C,* total cell lysates were used to monitor the level of phosphorylated AKT (pAKT^{T308} and pAKT^{S473}), MEK1/2 (pMEK1/2), and ERK1/2 (pERK1/2) proteins.

obtained revealed that substitution of Trp-79 for arginine in E-RAS (E-RAS^{Arg-79}) rescued the low affinity of E-RAS for PLCε, RAF1, and RalGDS, and no effect was observed on RASSF5 binding (Fig. 3*B*). In contrast, W79R-containing variants (E-RAS^{Arg-79}, E-RAS$^{SwI/Arg-79}$, E-RAS$^{Arg-79/SwII}$, and E-RAS$^{SwI/Arg-79/SwII}$), when compared with E-RAS^{WT}, exhibited a significant reduction of binding affinity for PI3Kα, which is comparable with the levels with H-RAS^{Val-12}. Collectively, all mutations in three regions, especially W79R, affected E-RAS interaction for PI3Kα (Fig. 3*B*). Mutations in the switch I region (E-RAS^{SwI}, E-RAS$^{SwI/Arg-79}$, RAS$^{SwI/SwII}$, and E-RAS$^{SwI/Arg-79/SwII}$) exclusively compromised E-RAS interaction with RASSF5. However, switch II variants (E-RAS^{SwII}, E-RAS$^{Arg-79/SwII}$, and RAS$^{SwI/SwII}$) more strongly diminished affinity for RalGDS and RAF1 (Fig. 3*B*).

These results raised the following question. How does the Trp-79 interaction with effectors affect the binding affinity of E-RAS for these proteins? To address this question, we inspected available H-RAS structures in complexes with investigated effector proteins and created corresponding structural models of E-RAS with particular focus on Trp-79 in E-RAS (Arg-41 in H-RAS). Data obtained pointed to an unexpected and potentially significant role of Glu-3 (Glu-41 in E-RAS) in effector selection by RAS proteins (Fig. 4; supplemental Fig. S1). Arg-41 is stabilized by intramolecular interactions with Glu-3 (Glu-41 in E-RAS) and side-chain contacts directly at Lys-65 of RAF1 among the analyzed H-RAS effector complexes but not PI3K. Tryptophan replacing Arg-41 in E-RAS would, because of its hydrophobic nature, be expelled from Glu-41, Glu-54, and Asn-92. This generates new conformation in the effector region of E-RAS and accounts for a shift in effector selectivity. The highest probability for such adopting provides an empty space around the Arg-41 in the case of the PI3K complex thus yielding higher affinity of PI3K to E-RAS^{WT}. Trp-79 interacts best in a hydrophobic environment with PI3K as compared with RAF1. Reciprocal scenario applies in the case of RAF1 and PLCε causing lower affinity of these effectors to E-RAS^{WT}. One example is the repulsion of Lys-65 of RAF1 by the W79R mutation that might be responsible for a weak reconstitution of E-RAS^{Arg-79} binding to RAF1.

We next examined the consequences of the affected effector interaction of the E-RAS variants regarding activation of the corresponding downstream cascades (see Fig. 3*C*). Interestingly, impaired PI3Kα binding of E-RAS variants, particularly W79R and SwII, also strongly influenced downstream signals of PI3K monitored by pAKT levels but not that of RAF1 analyzed by pMEK/pERK levels (Fig. 3*C*). Remarkably, AKT phosphorylation at both sides, Thr-308 (PDK1) and Ser-473 (mTORC2), were impaired (see below). The E-RAS^{Arg-79} variant lost its ability to signal via the PI3K/AKT cascade almost completely, indicating a key role of tryptophan 79 in E-RAS and E-RAS-like proteins in effector association and activation. An interesting observation is that a gain of RAF1 binding to E-RAS variants, especially SwI and W79R, did not result in RAF1 activation and

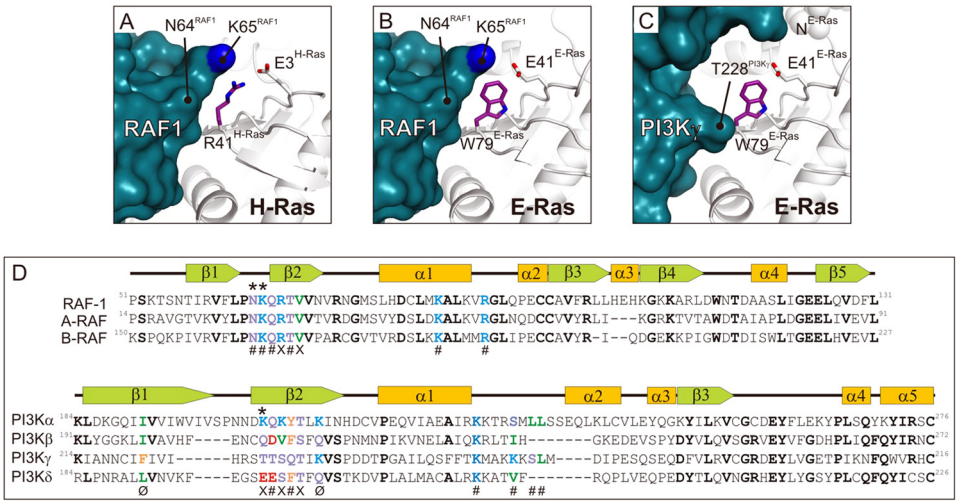

FIGURE 4. **Glutamate 41 function and its role in effector selection is discharged in E-RAS.** *A,* in H-RAS-GTP, Arg-41 (Trp-79 in E-RAS) is intramolecularly stabilized by Glu-3 (Glu-41 in E-RAS), attracted by backbone oxygen of Asn-64, and repulsed by Lys-65 in RAF1. *B,* in E-RAS, Trp-79 is expelled from Glu-41 and cannot adopt favorable conformation because of the close presence of Asn-64 and Lys-65 of RAF1. The conformation of arginine at the place of Trp-79 in E-RAS^{Arg-79} would be restored due to its interaction with Glu-41 similarly to H-RAS, thus increasing the binding affinity of RAF1. *C,* PI3K does not contact E-RAS tightly in the vicinity of Trp-79 leaving enough space for proper reorientation of tryptophan side chain expelled from Glu-41 and not disfavoring the affinity of their complex. Moreover, orientation of Thr-228 enables tight hydrophobic contact with Trp-79. In E-RAS^{Arg-79}, arginine attracted by Glu-41 would not contribute to the interaction with PI3K weakening its affinity to E-RAS^{Arg-79}. *D,* selectivity-determining amino acids in RAS effectors. Multiple amino acid sequence alignments of the RBD of human RAF isoforms and the catalytic subunits of human PI3K isoforms are illustrated with major focus on the some RAS-binding residues. The corresponding sequences are RAF-1 (P04049; aa 51–131), A-RAF (P10398; aa 14–91), B-RAF (P15056; aa 105–227), PI3Kα (P42336; aa 184–276), PI3Kβ (P42338; aa 191–272), PI3Kγ (P48736; aa 214–296), and PI3Kδ (O00329; aa 184–226). *X* highlights residues interacting in β-β manner with switch I. # highlights additional residues interacting with switch I. Ø shows residues interacting with Tyr-64 in switch II. * shows residues close to Arg-41 in H-RAS or Trp-79 in E-RAS.

in turn phosphorylation of MEK1/2 and ERK1/2 (Fig. 3, *B* and *C*).

Distinct Downstream Signaling Pathways of E-RAS via PI3K—The data presented above shed light on the specificity determining residues for direct E-RAS-effector interaction and the consequent activation of downstream pathways. The next question we addressed was to understand the role of additional motifs within the N-terminal extension and HVR of E-RAS (see Fig. 1*A*) as potential molecular and cellular determinants required for signal transduction through PI3K-AKT-mTORC and RAF1-MEK1/2-ERK1/2. Therefore, we first investigated the ability of E-RAS variants to directly interact with PI3Kα and RAF1. In this experiment, FLAG-tagged E-RAS variants, H-RAS^{WT} and H-RAS^{Val-12}, transiently transfected in COS-7 cells, were pulled down with GST-fused PI3Kα-RBD and RAF1-RBD from the cell lysates (Fig. 5*A*). Similar to E-RAS^{WT}, the interactions of E-RAS variants were much stronger with PI3Kα-RBD as compared with RAF1-RBD, although hyperactive H-RAS^{Val-12} mainly bound to RAF1-RBD. Moreover, this assay was used to visualize the amounts of the GTP-bound state of the E-RAS variants. Fig. 5*A* shows that all E-RAS variants exist in the active, GTP-bound forms.

To provide further insights to the downstream signaling activity of the above-mentioned E-RAS variants, we investigated the phosphorylation status of AKT (Thr-308 and Ser-473), MEK1/2 (Ser-217/Ser-221), and ERK1/2 (Thr-202/Thr-204), which are representative cellular targets of PI3K and RAF1 (Fig. 5*B*). Although the pulldown showed almost no significant difference between E-RAS variants in binding to RAS effectors, we found E-RAS$^{\Delta N}$, E-RAS$^{Ser-226/Ser-228}$, and E-RAS$^{\Delta N/Ser-226/Ser-228}$ were strongly impaired in the activation of the PI3K-AKT-mTORC axis and clearly exhibited lower phosphorylation levels for AKT, especially at Thr-308. All E-RAS variants, including E-RAS$^{\Delta N}$, were inefficient in stimulation of MEK1/2 and ERK1/2 phosphorylation in comparison with H-RAS^{WT} and H-RAS^{Val-12} that actively contributed to activation of the RAF1-MEK1/2-ERK1/2 axis.

Next, we aimed to determine the cellular co-localization of E-RAS with PI3Kα and RAF1. Transiently transfected MDCK II cells with FLAG-tagged E-RAS and H-RAS were incubated with recombinant GST-fused RBDs of PI3Kα and RAF1 and stained with antibodies against GST and FLAG, respectively. We observed that PI3Kα but not RAF1 localized with E-RAS mainly at the plasma membrane (Fig. 6*A*). In contrast, RAF1, and to a lower extent also PI3Kα, co-localized with H-RAS at the plasma membrane (Fig. 6*B*). These data suggest that both the N-terminal extension of E-RAS and its palmitoylation are essential and critical for the cellular activation of the PI3K-AKT-mTORC cascade, although the formation of the GTP-bound state and the interaction with PI3K were not affected.

Discussion

In this study, we have investigated cellular localization and the signaling activity of human E-RAS regarding its physical interaction with RAS effectors and the roles of both its unique features, the N terminus and PTM by palmitoylation in direct comparison with human H-RAS. The structure-function relationship of the effector interaction sites of E-RAS resulted in the identification of tryptophan 79 as a specificity-determining amino acid of E-RAS, which is critical for its strong association with PI3K. In the cell, this interaction additionally requires the presence of both a functional N-terminal extension and palmitoylation at cysteines 226 and 228 that collectively lead to the precise activation of the PI3K-AKT-mTORC pathway.

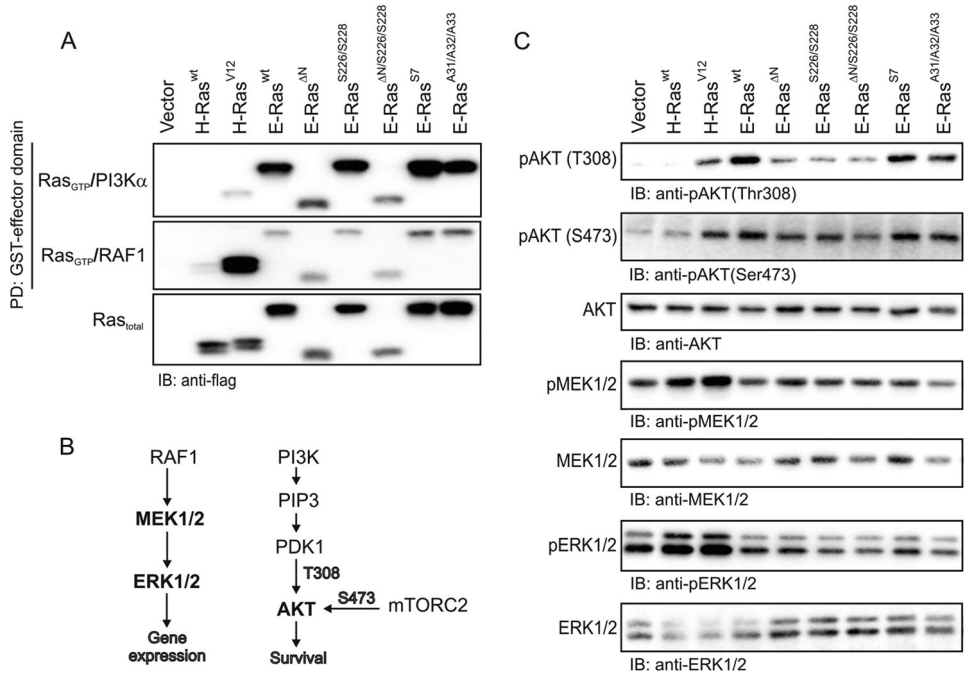

FIGURE 5. **E-RAS signaling activities in COS-7 cells.** Pulldown (*PD*) experiments and immunoblot (*IB*) analysis of total cell lysates were derived from transfected COS-7 cells with FLAG-tagged E-RAS variants H-RAS^{WT} and H-RAS^{Val-12}. *A,* pulldown analysis revealed that E-RAS variants like E-RAS^{WT} most strongly bind to GST-fused PI3Kα-RBD than RAF1-RBD, whereas hyperactive H-RAS^{Val-12} mainly bound to GST-fused RAF1-RBD. In addition, PI3Kα-RBD PD showed that all E-RAS variants are in the GTP-bound state and consequently in their activated forms. Total amounts of the RAS proteins were detected as a control using anti-FLAG antibody. *B,* schematic view of MAPK and PI3K-AKT cascades. *C,* total cell lysates were analyzed for the phosphorylation level of AKT (pAKT308 and pAKT473), MEK1/2 (pMEK1/2) and ERK1/2 (pERK1/2). Total amounts of AKT, MEK1/2, and ERK1/2 were applied as loading controls.

Palmitoylation Modification and E-RAS Trafficking—To transduce signals, RAS proteins should be associated with the lipid membranes. They are compartmentalized by PTMs at their C terminus, with the C*AAX* motif at the farnesylation site, and additional upstream cysteine residues at the palmitoylation site(s) in the case of H- and N-RAS (supplemental Fig. S1) (23–25, 29). We found that like the mouse E-RAS (42), substitution of two cysteine residues Cys-226/Cys-228 in HVR of human E-RAS with serines clearly impaired the plasma membrane localization of protein. This is a strong indication that human E-RAS undergoes palmitoylation at these sites, as described for the first time for H-RAS (62). Yamanaka and co-workers (42) reported that these cysteine residues are important for endomembrane localization of mouse E-RAS and only signals if HVR of H-RAS can rescue endomembrane localization of E-RAS$^{Ser-226/Ser-228}$. Our confocal microscopy data revealed that in contrast to plasma membrane localization of E-RAS^{WT}, palmitoylation-deficient E-RAS$^{Ser-226/Ser-228}$ is mainly localized, with a clear pattern, in cytoplasm and also in endomembranes. Our data clearly support proposed reports demonstrating that H-RAS and N-RAS cycle between Golgi and the plasma membrane via reversible and dynamic palmitoylation-depalmitoylation reactions (25, 63, 64).

N-terminal Extension and C-terminal Insertion of E-RAS—A sequence comparison between E-RAS and other RAS isoforms highlighted additional regions and motifs, such as the unique N terminus of E-RAS that is not present in other RAS-like proteins. We propose that the N-terminal extension of E-RAS might modulate its localization through interaction with potential adaptor/scaffold proteins via putative P*XX*P and RRR motifs. With our co-localization studies, we did not observe significant differences in localization of the N-terminal mutants of E-RAS. However, considering our results, we cannot exclude the role of the E-RAS N terminus as a putative protein interaction site, because E-RAS is not expressed endogenously in the MDCK II cells, and therefore its binding partner may not be available in this cell line. To confirm our hypothesis, we need to study a different cell line, like embryonic stem cells (42), gastric tumors (65), neuroblastoma cells (20), and also hepatic stellate cells,[3] where E-RAS is endogenously expressed (unpublished data).

Imaging methods used in this study did not allow visualizing microdomain localization of E-RAS variants. The plasma membrane is not a homogeneous lipid bilayer and includes a set of microdomains, such as lipid raft and caveolae (66, 67). The HVR at the C-terminal end of RAS proteins is critical for lateral sorting and is divided into two separate domains, membrane-targeting domain and linker domain (68). Membrane targeting domain contains a C*AAX* box and one or two upstream cysteines that are palmitoylation sites. Palmitoylated proteins can be targeted to lipid rafts. Because H-, N-, and K-RAS are dipalmitoylated, monopalmitoylated, and nonpalmitoylated, respectively, they exhibit different lateral segregation across the plasma membrane microdomains (69). GDP-bound H-RAS is associated with the lipid raft, but when it is activated and GTP-loaded, it moves laterally to nonlipid raft regions (68, 70, 71). E-RAS, like H-RAS, is dipalmitoylated suggesting that it may favor the lipid rafts. On the contrary, E-RAS is mainly GTP-

[3] S. Nakhaei-Rad, C. Kordes, H. Nakhaeizadeh, R. Dvorsky, I. C. Cirstea, I. Sawitza, S. Götze, Ro. P. Piekorz, B. Görg, D. Haussinger, and M. R. Ahmadian, unpublished data.

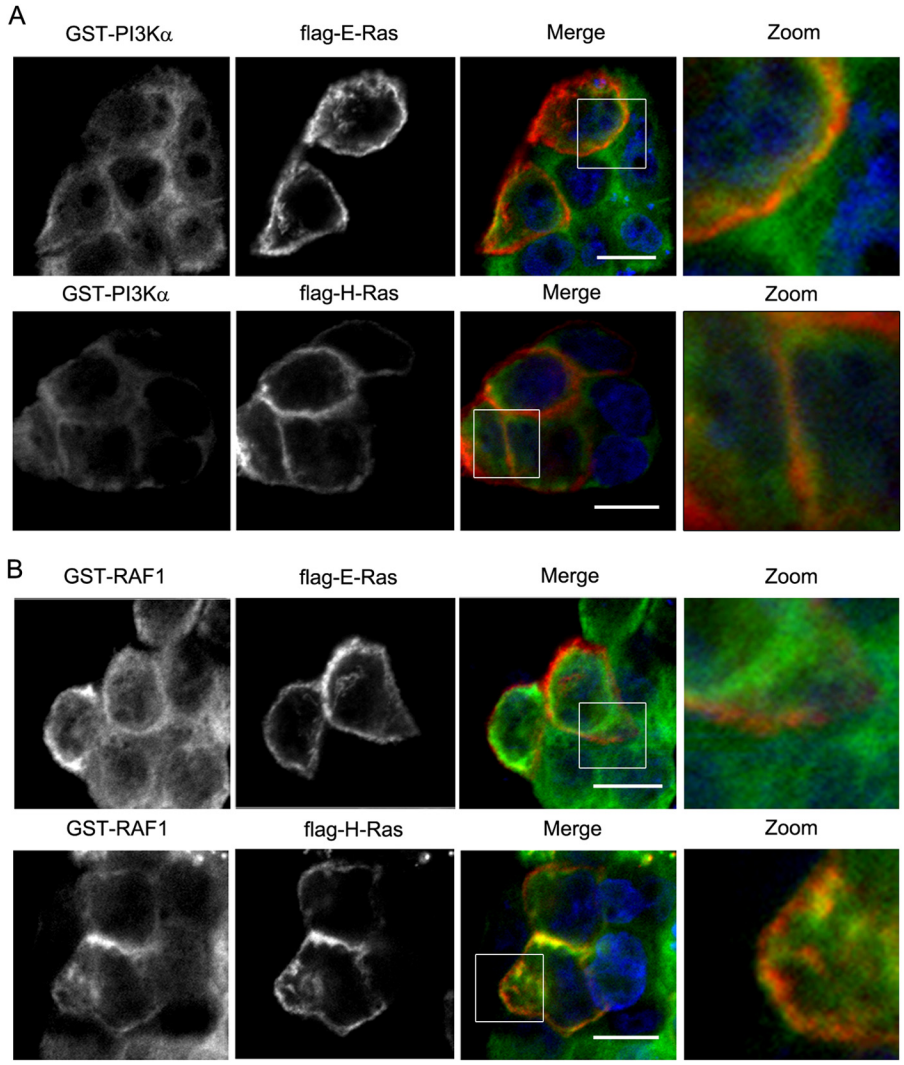

FIGURE 6. **Co-localization of E-RAS with PI3Kα.** Transfected MDCKII cells with FLAG-tagged E-RAS were incubated with bacterial lysates, containing GST-RBDs of PI3Kα and RAF1 proteins and stained with antibodies raised against GST and FLAG to investigate their co-localization with GTP-bound H-RAS and E-RAS proteins. E-RAS co-localized with PI3Kα. *Scale bar,* 10 μm.

loaded, which makes it difficult to compare it with wild-type H-RAS. It is reported that the active GTP-loaded H-RAS$^{Val\text{-}12}$ variant occupies the nonlipid rafts so the constitutively active E-RAS may also be clustered in this region. The second domain in HVR, termed linker domain, releases GTP-loaded H-RAS from the lipid rafts. Linker domain can be divided in N- and C-terminal regions in a way that the C-terminal region is a spacer, which seems not to be important (68). Human E-RAS has an insertion in this C-terminal spacer (aa 173–179, H-RAS numbering) that may also affect microdomain migration of E-RAS. Taken together, we propose that three factors most likely modulate the microdomain targeting of E-RAS, such as an extended N terminus, a C-terminal insertion, and the GTP-loaded state due to a prominent deviation at position Ser-50 (Gly-12 in H-RAS).

Our cell-based studies revealed that the N-terminal extension of E-RAS is critical for PI3K-AKT-mTORC activation, and N-terminal truncated E-RAS variants (E-RAS$^{\Delta N}$ and E-RAS$^{\Delta N/Ser\text{-}226/Ser\text{-}228}$) remarkably had a lower signaling activity. One explanation may be the role of the unique N terminus in the lateral segregation of E-RAS across the membrane that consequently specifies association with and activation of its effectors in a manner reminiscent to microdomain localization of H-RAS that regulates its interaction with effector proteins of RAF1 and PI3K (68). In addition, E-RAS was found in membrane ruffles (data not shown), which may be induced by Rac1 activated by the E-RAS-PI3K-PIP_3-RacGEF axis (72–74). Such a scenario has been reported for the R-RAS N-terminal 26-amino acid extension, which has been proposed to positively regulate Rac activation and cell spreading (75).

Constitutively Active Form—GAPs accelerate the GTP hydrolysis reaction of RAS proteins by orders of magnitude by supplying a highly conserved, catalytic arginine finger (31, 32). H-RAS glycine 12 mutations to any other amino acid interfere with insertion of arginine finger in the GTPase active site and therefore make the enzyme GAP-insensitive (30). Interestingly, E-RAS has a deviation in the corresponding position and carries a serine instead of a glycine indicating that E-RAS is hyperactive and GAP-insensitive. Our stopped-flow data revealed that p120RASGAP was not able to accelerate the GTP hydrolysis

reaction of E-RAS, although it can act on H-RAS and convert it to the GDP-bound inactive form (data not shown). We have shown that all E-RAS variants exist mostly in GTP-bound forms as shown by a pulldown experiment with PI3K and RAF1. This and the fact that E-RAS is GAP-insensitive suggest that E-RAS may underlie a different and yet undefined control mechanism that negatively regulates E-RAS activity and thus its signal transduction.

It seems that expression of E-RAS is highly regulated at the transcriptional levels and rather limited to special cell types, such as embryonic stem cells (42), gastric tumors (65), neuroblastoma cells (20), and also hepatic stellate cells.[5] Moreover, the unique N terminus of E-RAS may provide specialized protein-protein interaction sites resulting in E-RAS sequestration, degradation, or membrane microdomain localization as shown for R-RAS (75, 76). E-RAS could interact with specific scaffolding proteins that bring it close to its effectors and regulate its activities. It is tempting to speculate that E-RAS may underlie a similar mechanism via serine/threonine phosphorylation and 14-3-3 binding as described for Rnd3 (75, 76), a constitutively active member of the Rho protein family (77). However, there is as yet no evidence for an E-RAS phosphorylation particularly at its N terminus that contains 4 threonines and 2 serines (supplemental Fig. S1).

Effector Binding Regions—RAS proteins transduce extracellular signals to a variety of intracellular signaling pathways through the interaction with a wide spectrum of effector proteins. Upon GDP to GTP exchange, RAS proteins undergo conformational changes in two critical regions, switch I and switch II. Notably, the GTP-bound form of RAS interacts with their target effectors through switch regions and thereby activates various pathways (5). A detailed study of structure-sequence relationships revealed a distinctive effector binding region for E-RAS in comparison with RAS isoforms (H-, N-, and K-RAS). Subsequent interaction analysis with five different RAS effectors revealed that effector binding profile of E-RAS significantly differs from H-RAS. E-RAS^{WT} tightly bound to PI3Kα and revealed very low affinity for other RAS effectors. In contrast, H-RAS showed an opposite pattern with the highest affinity for RAF1. These data were confirmed by investigating the respective downstream signaling cascades (PI3K-AKT-mTORC and RAF1-MEK1/2-ERK1/2) at the level of phosphorylated AKT, MEK1/2, and ERK1/2. Our results are consistent with a previous study of Yamanaka and co-workers (18), who applied another PI3K isoform (PI3Kδ) and observed differences between H-RAS and E-RAS. It seems probable that E-RAS and H-RAS possess a different affinity for distinct PI3K isoforms, α, β, γ, and δ, and this may account for their specific biological outputs (78). Consistently, the catalytic subunit of the PI3Kγ isoform, PI3Kγ, interacts with switch I of H-RAS in anti-parallel β-sheet fashion (48), also approaching RAS-conserved Asp-33 by two lysines. Residues in H-RAS contacting β-strand of PI3Kγ and preceding amino acids differ significantly among the PI3K isoforms regarding the primary structures (Fig. 4*D*). Although PI3Kγ has four hydroxyl-containing amino acid side chains at this place, PI3Kβ possesses one and PI3Kδ isoform two negatively charged residues whereby both have in addition two amino acid insertions. In contrast, the PI3Kα isoform has insertion of six residues, and the hydroxyl-containing amino acids are replaced by one asparagine and two lysines (Fig. 4*D*). We hypothesize that these differences in PI3K isoforms are of particular importance due to the stabilization of intermolecular β-sheet interaction and especially because the contact site of the crucial Trp-79 in E-RAS (Arg-41 in H-RAS) is highly variable (Lys, Gln, Thr, and Glu; see Fig. 4*D*).

Substitutions for E-RAS residues in the switch I and II and interswitch regions with corresponding residues in H-RAS provided several interesting aspects and new insights (Fig. 3). One is a shift in effector selection. Strikingly, and in contrast to other investigated effectors, RAF1-RBD undergoes contacts with the switch I and the interswitch regions (Fig. 2*A*) (46, 47). However, E-RAS^{SwI}, which has an almost identical switch I when compared with H-RAS, showed a reduced binding to RAF1 that was clearly elevated when this was combined with the interswitch mutation W79R (E-RAS$^{SwI/Arg\text{-}79}$) (Fig. 3*B*). Consistently, the major difference was observed with E-RAS$^{Arg\text{-}79}$, where a tryptophan was replaced by an arginine (Arg-41 in H-RAS). This variant led to increase in RAF1 binding and partly rescued the low affinity of the wild type and the switch variants (E-RAS$^{SwI/Arg\text{-}79}$ and E-RAS$^{SwI/Arg\text{-}79/SwII}$). According to the crystal structure (46), Arg-41 in H-RAS (Trp-79 in E-RAS) interestingly forms a hydrogen bond with the backbone oxygen of Asn-64 in RAF1-RBD that very likely enabled E-RAS$^{Arg\text{-}79}$ to make additional electrostatic contacts with RAF1 (Fig. 4, *A* and *B*). In addition, E-RAS shares a glutamate (Glu-41) with H-RAS (Glu-3) (supplemental Fig. S1). Glu-3 interacts in intermolecular fashion with Arg-41 and stabilizes the H-RAS·RAF1 complex formation (Fig. 4*A*). Accordingly, mutation of W79R in E-RAS reconstitutes such intermolecular interaction between Glu-41 and Arg-79, thus increasing significantly the interaction between E-RAS$^{Arg\text{-}79}$ and RAF1 (Fig. 3*B*). Another important contribution to effector binding concerning Trp-79 originates very likely in its expulsion from the above-mentioned Glu-41 and the ability of bound effector protein to accommodate altered conformation of Trp-79. As mentioned before, Arg-41 of H-RAS is contacted by RAF1 in its complex structure. The space where the tryptophan can be accommodated and hydrophobically interact with the effector is thus limited resulting in diminished affinity of these effectors to E-RAS^{WT}. Moreover, switch II quadruple mutation of E-RAS (E-RAS^{SwII}; see Fig. 3*A*) showed the largest impairment in RAF1 binding. This was not expected especially because the structural data, reported previously (46, 47), have shown that RAF1-RBD does not physically contact the switch II of RAS. Again, E-RAS$^{Arg\text{-}79/SwII}$ partially restored the loss of RAF1 binding but most remarkably not the E-RAS$^{SwI/SwII}$ variant that actually is almost identical to H-RAS regarding the amino acid sequence of its switch I and II regions (see Fig. 3*A*). Even though E-RAS$^{Arg\text{-}79}$ binds more tightly to RAF1, it still does not activate the MAPK pathway like E-RAS^{WT}. Note that there was no increase in MEK and ERK phosphorylation, and we detected even the opposite, namely a significant decrease in pMEK1/2 and pERK1/2 as compared with the vector control (Fig. 3*C*; see *E-RAS^{WT}* and *E-RAS$^{Arg\text{-}79}$ lanes*). An explanation for the absence of E-RAS$^{Arg\text{-}79}$ signaling toward the MAPK pathway is that most probably the additional component, including scaffold proteins such as SHOC2 (79–

81), may not exist in the E-RAS^{Arg-79}·RAF1 complex. This provides the assumption that E-RAS localizes to a different membrane region then, for example, the H-RAS, RAF1, and the components of the MAPK pathway.

PLCϵ contains two RAS association domains, RA1 and RA2. RA2 forms a complex with H-RAS in a GTP-dependent manner by contacting nine different residues of the switch I and II regions, and also Gln-25 and Arg-41 (51), from which four (Glu-37, Arg-41, Glu-63, and Tyr-63) deviate in E-RAS (Fig. 3*A*). This explains why we observed an extremely weak E-RAS-PLCϵ interaction as compared with H-RAS^{Val-12}. Most interestingly, the W79R mutation of E-RAS resulted in a strong gain of binding activity (Fig. 3*B*; see *E-RAS^{WT}* and *E-RAS^{Arg-79} lanes*). Notably, this effect was not so strong in the case of the switch II mutation (E-RAS^{SwII}), and the switch I mutation (E-RAS^{SwI}) did not show any change in the E-RAS association with PLCϵ. A combination of the mutations (E-RAS$^{SwI/SwII}$) was hardly detectable and the combinations with W79R (E-RAS$^{Arg-79/SwI}$, E-RAS$^{Arg-79/SwII}$, and RAS$^{SwI/Arg-79/SwII}$) rather counteracted the gain of binding activity of RAS^{Arg-79}. On a molecular level, Trp-79 in wild-type E-RAS can be hydrophobically attracted to Pro-2149 of PLCϵ but not intramolecularly to Glu-41 (data not shown), and the space for its conformational relaxation is limited similarly to RAF1 as mentioned above. We propose that W79R mutation generates stronger intramolecular contact between Glu-41 and Arg-79 and consequently stabilizes the protein complex with PLCϵ. Katan and co-workers (51) have discussed that the H-RAS residues Tyr-64, Ile-36, and Met-67 (His-102, Ile-74, and Leu-105 in E-RAS) in combination with Phe-2138 and Val-2152 from PLCϵ-RA2, provide a hydrophobic clusters. Introduction of another hydrophobic residue in E-RAS as demonstrated with a single point mutation at Trp-79 (E-RAS^{Arg-79}) has obviously created an additional and distinct binding site for RAS association domains, such as RA2 of PLCϵ and most likely also RA of RalGDS. The latter, a GEF for Ral, links two RAS family members, RAS and Ral (82). Although the crystal structure of H-RAS/RalGDS-RA has not reported an involvement of Arg-41 (50), our structural analysis predicted a close hydrophobic contact of Arg-41 with Met-819 of RalGDS (3.2 Å). Notably, data obtained from the interaction of RalGDS and RAF1 with E-RAS variants appear similar as compared with that for PLCϵ.

PI3K is a well known effector of classical RAS proteins and promotes cellular survival (78). In comparison with H-RAS, E-RAS interacts more strongly with PI3Kα-RBD and activates the PI3K-AKT-mTORC cascade. Mutagenesis at switch and interswitch regions (E-RAS^{SwI}, E-RAS^{Arg-79}, and E-RAS^{SwII}), attenuated binding of E-RAS to PI3Kα-RBD, demonstrating the role of critical E-RAS residues at effector binding regions. These data are consistent with a previous study that has shown that PI3Kγ-RBD contacts both switch I and switch II regions of H-RAS (48). Interestingly, W79R mutation of E-RAS (Arg-41 H-RAS), which has increased binding to RAF1, PLCϵ, and RalGDS, dramatically reduced the binding to PI3Kα. The affinity of this E-RAS mutant (E-RAS^{Arg-79}) for PI3Kα-RBD appears similar to that of H-RAS^{Val-12} (Fig. 3*B*; see *H-RAS^{Val-12}* and *E-RAS^{Arg-79} lanes*). We think that the strong interaction between E-RAS and PI3K stems from the ability of structure to accommodate altered conformation of Trp-79 and from its hydrophobic contact to PI3K (Fig. 4*C*). In contrast, W79R mutation in E-RAS enables Glu-41 to attract Arg-79 and to interfere with this hydrophobic interaction, resulting in a significant reduction of the binding affinity between PI3K and E-RAS (Fig. 4*C*). In the same line of evidence, we also observed E-RAS^{Arg-79} deficient at the activation of RAS-PI3K-AKT-mTORC2 pathway (9) as monitored with Ser-473 phosphorylation of AKT (see result Fig. 3*C*). Thus, Trp-79 in E-RAS represents a specificity-determining residue for the proper binding to and activation of PI3K.

RASSF members are known as a RAS effector with tumor suppressor functions. RASSF5 have two splice variants NORE1A and RAPL, which share same RBD (53). We applied the RASSF5-RA domain to analyze the interaction of E-RAS variants with this RAS effector. As shown for RAF1 and RalGDS, switch I H70Y/Q75E mutation of E-RAS (E-RAS^{SwI}) also attenuated the binding to RASSF5, and this was the case for all E-RAS variants harboring switch I mutations (E-RAS$^{SwI/Arg-79}$, E-RAS$^{SwI/SwII}$, and E-RAS$^{SwI/Arg-79/SwII}$). Switch II and W79R mutations did not affect the binding affinity for RASSF5, emphasizing the importance of the more conserved switch I region in the complex formation of the RAS proteins with RASSF5 (53). It remains to be investigated whether E-RAS is an activator of RASSF5 and thus a regulator of the Hippo pathway.

In summary, we conclude that switch regions of E-RAS act as core effector binding regions that form an E-RAS-specific interaction interface for its effectors, such as PI3K. The PI3K isoform specificity in E-RAS-expressing cells remains to be investigated. Trp-79 of E-RAS appears to determine the effector selectivity. E-RAS binding to other RAS effectors, such as RASSF5, RalGDS, and RAF1, is weak but may still be of physiological relevance. Improvement of the interaction with RAF1 by mutagenesis, for example, rather exhibited an inhibitory impact on the MAPK pathway. It remains unclear whether protein phosphatases specific for MAPKs were activated. The N terminus of E-RAS is unique and may play a critical role in the interaction with its accessory proteins for positioning E-RAS to subcellular microdomains of the plasma membrane.

Acknowledgments—We are grateful to Ehsan Amin, Hedyeh Amintoosi, Silke Götze, Lothar Gremer, Ilse Meyer, Kazem Nouri, Björn Papke, Roland P. Piekorz, Georg Rosenberger, Claudia Rupprecht, Iris Sawitza, Jürgen Scheller, Madhurendra Singh, Nachiket Vartak, and Si-Cai Zhang for their helpful advice, stimulating discussions, and for sharing reagents.

Note Added in Proof—Supplemental Fig. 1 comparing mammalian E-RAS and classical RAS sequences was inadvertently omitted from the version of this article that was published May 4, 2015 as a Paper in Press. Supplemental Fig. 1 is now available on line.

References

1. Vetter, I. R. (2001) The guanine nucleotide-binding switch in three dimensions. *Science* **294,** 1299–1304
2. Boguski, M. S., and McCormick, F. (1993) Proteins regulating Ras and its relatives. *Nature* **366,** 643–654
3. Ahmadian, M. R., Wittinghofer, A., and Schmidt, G. (2002) The actin filament architecture: tightly regulated by the cells, manipulated by patho-

gens. International Titisee Conference on the actin cytoskeleton: from signalling to bacterial pathogenesis. *EMBO Rep.* **3,** 214–218
4. Gremer, L., Merbitz-Zahradnik, T., Dvorsky, R., Cirstea, I. C., Kratz, C. P., Zenker, M., Wittinghofer, A., and Ahmadian, M. R. (2011) Germ line KRAS mutations cause aberrant biochemical and physical properties leading to developmental disorders. *Hum. Mutat.* **32,** 33–43
5. Karnoub, A. E., and Weinberg, R. A. (2008) Ras oncogenes: split personalities. *Nat. Rev. Mol. Cell Biol.* **9,** 517–531
6. Pylayeva-Gupta, Y., Grabocka, E., and Bar-Sagi, D. (2011) RAS oncogenes: weaving a tumorigenic web. *Nat. Rev. Cancer* **11,** 761–774
7. Tidyman, W. E., and Rauen, K. A. (2009) The RASopathies: developmental syndromes of Ras/MAPK pathway dysregulation. *Curr. Opin. Genet. Dev.* **19,** 230–236
8. Flex, E., Jaiswal, M., Pantaleoni, F., Martinelli, S., Strullu, M., Fansa, E. K., Caye, A., De Luca, A., Lepri, F., Dvorsky, R., Pannone, L., Paolacci, S., Zhang, S. C., Fodale, V., Bocchinfuso, G., *et al.* (2014) Activating mutations in RRAS underlie a phenotype within the RASopathy spectrum and contribute to leukaemogenesis. *Hum. Mol. Genet.* **23,** 4315–4327
9. Cirstea, I. C., Gremer, L., Dvorsky, R., Zhang, S. C., Piekorz, R. P., Zenker, M., and Ahmadian, M. R. (2013) Diverging gain-of-function mechanisms of two novel KRAS mutations associated with Noonan and cardio-facio-cutaneous syndromes. *Hum. Mol. Genet.* **22,** 262–270
10. Castellano, E., and Santos, E. (2011) Functional specificity of Ras isoforms: so similar but so different. *Genes Cancer* **2,** 216–231
11. Ichise, T., Yoshida, N., and Ichise, H. (2010) H-, N- and Kras cooperatively regulate lymphatic vessel growth by modulating VEGFR3 expression in lymphatic endothelial cells in mice. *Development* **137,** 1003–1013
12. Omerovic, J., Laude, A. J., and Prior, I. A. (2007) Ras proteins: paradigms for compartmentalised and isoform-specific signalling. *Cell. Mol. Life Sci.* **64,** 2575–2589
13. Potenza, N., Vecchione, C., Notte, A., De Rienzo, A., Rosica, A., Bauer, L., Affuso, A., De Felice, M., Russo, T., Poulet, R., Cifelli, G., De Vita, G., Lembo, G., and Di Lauro, R. (2005) Replacement of K-Ras with H-Ras supports normal embryonic development despite inducing cardiovascular pathology in adult mice. *EMBO Rep.* **6,** 432–437
14. Leon, J., Guerrero, I., and Pellicer, A. (1987) Differential expression of the ras gene family in mice. *Mol. Cell. Biol.* **7,** 1535–1540
15. Johnson, L., Greenbaum, D., Cichowski, K., Mercer, K., Murphy, E., Schmitt, E., Bronson, R. T., Umanoff, H., Edelmann, W., Kucherlapati, R., and Jacks, T. (1997) K-ras is an essential gene in the mouse with partial functional overlap with N-ras. *Genes Dev.* **11,** 2468–2481
16. Nakamura, K., Ichise, H., Nakao, K., Hatta, T., Otani, H., Sakagami, H., Kondo, H., and Katsuki, M. (2008) Partial functional overlap of the three ras genes in mouse embryonic development. *Oncogene* **27,** 2961–2968
17. Lau, K. S., and Haigis, K. M. (2009) Nonredundancy within the RAS oncogene family: insights into mutational disparities in cancer. *Mol. Cells* **28,** 315–320
18. Takahashi, K., Mitsui, K., and Yamanaka, S. (2003) Role of ERas in promoting tumour-like properties in mouse embryonic stem cells. *Nature* **423,** 541–545
19. Tanaka, Y., Ikeda, T., Kishi, Y., Masuda, S., Shibata, H., Takeuchi, K., Komura, M., Iwanaka, T., Muramatsu, S., Kondo, Y., Takahashi, K., Yamanaka, S., and Hanazono, Y. (2009) ERas is expressed in primate embryonic stem cells but not related to tumorigenesis. *Cell Transplant.* **18,** 381–389
20. Aoyama, M., Kataoka, H., Kubota, E., Tada, T., and Asai, K. (2010) Resistance to chemotherapeutic agents and promotion of transforming activity mediated by embryonic stem cell-expressed Ras (ERas) signal in neuroblastoma cells. *Int. J. Oncol.* **37,** 1011–1016
21. Kubota, E., Kataoka, H., Aoyama, M., Mizoshita, T., Mori, Y., Shimura, T., Tanaka, M., Sasaki, M., Takahashi, S., Asai, K., and Joh, T. (2010) Role of ES cell-expressed Ras (ERas) in tumorigenicity of gastric cancer. *Am. J. Pathol.* **177,** 955–963
22. Willumsen, B. M., Christensen, A., Hubbert, N. L., Papageorge, A. G., and Lowy, D. R. (1984) The p21 ras C-terminus is required for transformation and membrane association. *Nature* **310,** 583–586
23. Ahearn, I. M., Haigis, K., Bar-Sagi, D., and Philips, M. R. (2012) Regulating the regulator: post-translational modification of RAS. *Nat. Rev. Mol. Cell Biol.* **13,** 39–51
24. Schmick, M., Vartak, N., Papke, B., Kovacevic, M., Truxius, D. C., Rossmannek, L., and Bastiaens, P. I. (2014) KRas localizes to the plasma membrane by spatial cycles of solubilization, trapping and vesicular transport. *Cell* **157,** 459–471
25. Rocks, O., Peyker, A., Kahms, M., Verveer, P. J., Koerner, C., Lumbierres, M., Kuhlmann, J., Waldmann, H., Wittinghofer, A., and Bastiaens, P. I. (2005) An acylation cycle regulates localization and activity of palmitoylated Ras isoforms. *Science* **307,** 1746–1752
26. Takahashi, K., Murakami, M., and Yamanaka, S. (2005) Role of the phosphoinositide 3-kinase pathway in mouse embryonic stem (ES) cells. *Biochem. Soc. Trans.* **33,** 1522–1525
27. Yu, Y., Liang, D., Tian, Q., Chen, X., Jiang, B., Chou, B.-K., Hu, P., Cheng, L., Gao, P., Li, J., and Wang, G. (2014) Stimulation of somatic cell reprogramming by ERas-Akt-FoxO1 signaling axis. *Stem Cells* **32,** 349–363
28. Lerner, E. C., Qian, Y., Blaskovich, M. A., Fossum, R. D., Vogt, A., Sun, J., Cox, A. D., Der, C. J., Hamilton, A. D., and Sebti, S. M. (1995) Ras CAAX peptidomimetic FTI-277 selectively blocks oncogenic Ras signaling by inducing cytoplasmic accumulation of inactive Ras-Raf complexes. *J. Biol. Chem.* **270,** 26802–26806
29. Apolloni, A., Prior, I. A., Lindsay, M., Parton, R. G., and Hancock, J. F. (2000) H-ras but not K-ras traffics to the plasma membrane through the exocytic pathway. *Mol. Cell. Biol.* **20,** 2475–2487
30. Scheffzek, K., Ahmadian, M. R., Kabsch, W., Wiesmüller, L., Lautwein, A., Schmitz, F., and Wittinghofer, A. (1997) The Ras-RasGAP complex: structural basis for GTPase activation and its loss in oncogenic Ras mutants. *Science* **277,** 333–338
31. Ahmadian, M. R., Hoffmann, U., Goody, R. S., and Wittinghofer, A. (1997) Individual rate constants for the interaction of Ras proteins with GTPase-activating proteins determined by fluorescence spectroscopy. *Biochemistry* **36,** 4535–4541
32. Ahmadian, M. R., Stege, P., Scheffzek, K., and Wittinghofer, A. (1997) Confirmation of the arginine-finger hypothesis for the GAP-stimulated GTP-hydrolysis reaction of Ras. *Nat. Struct. Biol.* **4,** 686–689
33. Lenzen, C., Cool, R. H., Prinz, H., Kuhlmann, J., and Wittinghofer, A. (1998) Kinetic analysis by fluorescence of the interaction between Ras and the catalytic domain of the guanine nucleotide exchange factor Cdc25Mm. *Biochemistry* **37,** 7420–7430
34. Buday, L., and Downward, J. (2008) Many faces of Ras activation. *Biochim. Biophys. Acta* **1786,** 178–187
35. Bourne, H. R., Sanders, D. A., and McCormick, F. (1990) The GTPase superfamily: a conserved switch for diverse cell functions. *Nature* **348,** 125–132
36. Bourne, H. R., Sanders, D. A., and McCormick, F. (1991) The GTPase superfamily: conserved structure and molecular mechanism. *Nature* **349,** 117–127
37. Saraste, M., Sibbald, P. R., and Wittinghofer, A. (1990) The P-loop–a common motif in ATP- and GTP-binding proteins. *Trends Biochem. Sci.* **15,** 430–434
38. Bos, J. L. (1989) ras oncogenes in human cancer: a review. *Cancer Res.* **49,** 4682–4689
39. Herrmann, C. (2003) Ras-effector interactions: after one decade. *Curr. Opin. Struct. Biol.* **13,** 122–129
40. Schmidt, G., Lenzen, C., Simon, I., Deuter, R., Cool, R. H., Goody, R. S., and Wittinghofer, A. (1996) Biochemical and biological consequences of changing the specificity of p21ras from guanosine to xanthosine nucleotides. *Oncogene* **12,** 87–96
41. Wittinghofer, A., and Vetter, I. R. (2011) Structure-function relationships of the G domain, a canonical switch motif. *Annu. Rev. Biochem.* **80,** 943–971
42. Takahashi, K., Nakagawa, M., Young, S. G., and Yamanaka, S. (2005) Differential membrane localization of ERas and Rheb, two Ras-related proteins involved in the phosphatidylinositol 3-kinase/mTOR pathway. *J. Biol. Chem.* **280,** 32768–32774
43. Tucker, J., Sczakiel, G., Feuerstein, J., John, J., Goody, R. S., and Wittinghofer, A. (1986) Expression of p21 proteins in *Escherichia coli* and stereochemistry of the nucleotide-binding site. *EMBO J.* **5,** 1351–1358
44. Cirstea, I. C., Kutsche, K., Dvorsky, R., Gremer, L., Carta, C., Horn, D.,

Roberts, A. E., Lepri, F., Merbitz-Zahradnik, T., König, R., Kratz, C. P., Pantaleoni, F., Dentici, M. L., Joshi, V. A., Kucherlapati, R. S., *et al.* (2010) A restricted spectrum of NRAS mutations causes Noonan syndrome. *Nat. Genet.* **42,** 27–29

45. Margarit, S. M., Sondermann, H., Hall, B. E., Nagar, B., Hoelz, A., Pirruccello, M., Bar-Sagi, D., and Kuriyan, J. (2003) Structural evidence for feedback activation by Ras. GTP of the Ras-specific nucleotide exchange factor SOS. *Cell* **112,** 685–695
46. Nassar, N., Horn, G., Herrmann, C., Block, C., Janknecht, R., and Wittinghofer, A. (1996) Ras/Rap effector specificity determined by charge reversal. *Nat. Struct. Biol.* **3,** 723–729
47. Filchtinski, D., Sharabi, O., Rüppel, A., Vetter, I. R., Herrmann, C., and Shifman, J. M. (2010) What makes Ras an efficient molecular switch: a computational, biophysical, and structural study of Ras-GDP interactions with mutants of Raf. *J. Mol. Biol.* **399,** 422–435
48. Pacold, M. E., Suire, S., Perisic, O., Lara-Gonzalez, S., Davis, C. T., Walker, E. H., Hawkins, P. T., Stephens, L., Eccleston, J. F., and Williams, R. L. (2000) Crystal structure and functional analysis of Ras binding to its effector phosphoinositide 3-kinase γ. *Cell* **103,** 931–943
49. Scheffzek, K., Grünewald, P., Wohlgemuth, S., Kabsch, W., Tu, H., Wigler, M., Wittinghofer, A., and Herrmann, C. (2001) The Ras-Byr2RBD complex: structural basis for Ras effector recognition in yeast. *Structure* **9,** 1043–1050
50. Huang, L., Hofer, F., Martin, G. S., and Kim, S. H. (1998) Structural basis for the interaction of Ras with RalGDS. *Nat. Struct. Biol.* **5,** 422–426
51. Bunney, T. D., Harris, R., Gandarillas, N. L., Josephs, M. B., Roe, S. M., Sorli, S. C., Paterson, H. F., Rodrigues-Lima, F., Esposito, D., Ponting, C. P., Gierschik, P., Pearl, L. H., Driscoll, P. C., and Katan, M. (2006) Structural and mechanistic insights into ras association domains of phospholipase Cϵ. *Mol. Cell* **21,** 495–507
52. Qamra, R., and Hubbard, S. R. (2013) Structural basis for the interaction of the adaptor protein grb14 with activated ras. *PLoS One* **8,** e72473
53. Stieglitz, B., Bee, C., Schwarz, D., Yildiz, O., Moshnikova, A., Khokhlatchev, A., and Herrmann, C. (2008) Novel type of Ras effector interaction established between tumour suppressor NORE1A and Ras switch II. *EMBO J.* **27,** 1995–2005
54. Vavvas, D., Li, X., Avruch, J., and Zhang, X. F. (1998) Identification of Nore1 as a potential Ras effector. *J. Biol. Chem.* **273,** 5439–5442
55. González-García, A., Pritchard, C. A., Paterson, H. F., Mavria, G., Stamp, G., and Marshall, C. J. (2005) RalGDS is required for tumor formation in a model of skin carcinogenesis. *Cancer Cell* **7,** 219–226
56. Castellano, E., and Downward, J. (2011) RAS interaction with PI3K: more than just another effector pathway. *Genes Cancer* **2,** 261–274
57. Bunney, T. D., and Katan, M. (2006) Phospholipase Cϵ: linking second messengers and small GTPases. *Trends Cell Biol.* **16,** 640–648
58. Yan, J., Roy, S., Apolloni, A., Lane, A., and Hancock, J. F. (1998) Ras isoforms vary in their ability to activate Raf-1 and phosphoinositide 3-kinase. *J. Biol. Chem.* **273,** 24052–24056
59. Song, C., Hu, C. D., Masago, M., Kariyai, K., Yamawaki-Kataoka, Y., Shibatohge, M., Wu, D., Satoh, T., and Kataoka, T. (2001) Regulation of a novel human phospholipase C, PLC, through membrane targeting by Ras. *J. Biol. Chem.* **276,** 2752–2757
60. Kuriyama, M., Harada, N., Kuroda, S., Yamamoto, T., Nakafuku, M., Iwamatsu, A., Yamamoto, D., Prasad, R., Croce, C., Canaani, E., and Kaibuchi, K. (1996) Identification of AF-6 and canoe as putative targets for Ras. *J. Biol. Chem.* **271,** 607–610
61. Lambert, J. M., Lambert, Q. T., Reuther, G. W., Malliri, A., Siderovski, D. P., Sondek, J., Collard, J. G., and Der, C. J. (2002) Tiam1 mediates Ras activation of Rac by a PI(3)K-independent mechanism. *Nat. Cell Biol.* **4,** 621–625
62. Hancock, J. F., Magee, A. I., Childs, J. E., and Marshall, C. J. (1989) All ras proteins are polyisoprenylated but only some are palmitoylated. *Cell* **57,** 1167–1177
63. Matallanas, D., Sanz-Moreno, V., Arozarena, I., Calvo, F., Agudo-Ibáñez, L., Santos, E., Berciano, M. T., and Crespo, P. (2006) Distinct utilization of effectors and biological outcomes resulting from site-specific Ras activation: Ras functions in lipid rafts and Golgi complex are dispensable for proliferation and transformation. *Mol. Cell. Biol.* **26,** 100–116
64. Goodwin, J. S., Drake, K. R., Rogers, C., Wright, L., Lippincott-Schwartz, J., Philips, M. R., and Kenworthy, A. K. (2005) Depalmitoylated Ras traffics to and from the Golgi complex via a nonvesicular pathway. *J. Cell Biol.* **170,** 261–272
65. Kaizaki, R., Yashiro, M., Shinto, O., Yasuda, K., Matsuzaki, T., Sawada, T., and Hirakawa, K. (2009) Expression of ERas oncogene in gastric carcinoma. *Anticancer Res.* **29,** 2189–2193
66. Simons, K., and Toomre, D. (2000) Lipid rafts and signal transduction. *Nat. Rev. Mol. Cell Biol.* **1,** 31–39
67. Iwabuchi, K., Handa, K., and Hakomori, S. (1998) Separation of "glycosphingolipid signaling domain" from caveolin-containing membrane fraction in mouse melanoma B16 cells and its role in cell adhesion coupled with signaling. *J. Biol. Chem.* **273,** 33766–33773
68. Jaumot, M., Yan, J., Clyde-Smith, J., Sluimer, J., and Hancock, J. F. (2002) The linker domain of the Ha-Ras hypervariable region regulates interactions with exchange factors, Raf-1 and phosphoinositide 3-kinase. *J. Biol. Chem.* **277,** 272–278
69. Prior, I. A., Muncke, C., Parton, R. G., and Hancock, J. F. (2003) Direct visualization of Ras proteins in spatially distinct cell surface microdomains. *J. Cell Biol.* **160,** 165–170
70. Prior, I. A., and Hancock, J. F. (2001) Compartmentalization of Ras proteins. *J. Cell Sci.* **114,** 1603–1608
71. Rotblat, B., Prior, I. A., Muncke, C., Parton, R. G., Kloog, Y., Henis, Y. I., and Hancock, J. F. (2004) Three separable domains regulate GTP-dependent association of H-ras with the plasma membrane. *Mol. Cell. Biol.* **24,** 6799–6810
72. Innocenti, M., Frittoli, E., Ponzanelli, I., Falck, J. R., Brachmann, S. M., Di Fiore, P. P., and Scita, G. (2003) Phosphoinositide 3-kinase activates Rac by entering in a complex with Eps8, Abi1, and Sos-1. *J. Cell Biol.* **160,** 17–23
73. Inabe, K., Ishiai, M., Scharenberg, A. M., Freshney, N., Downward, J., and Kurosaki, T. (2002) Vav3 modulates B cell receptor responses by regulating phosphoinositide 3-kinase activation. *J. Exp. Med.* **195,** 189–200
74. Dillon, L. M., Bean, J. R., Yang, W., Shee, K., Symonds, L. K., Balko, J. M., McDonald, W. H., Liu, S., Gonzalez-Angulo, A. M., Mills, G. B., Arteaga, C. L., and Miller, T. W. (2014) P-REX1 creates a positive feedback loop to activate growth factor receptor, PI3K/AKT and MEK/ERK signaling in breast cancer. *Oncogene* **6,** 328
75. Holly, S. P., Larson, M. K., and Parise, L. V. (2005) The unique N-terminus of R-ras is required for Rac activation and precise regulation of cell migration. *Mol. Biol. Cell* **16,** 2458–2469
76. Riou, P., Kjær, S., Garg, R., Purkiss, A., George, R., Cain, R. J., Bineva, G., Reymond, N., McColl, B., Thompson, A. J., O'Reilly, N., McDonald, N. Q., Parker, P. J., and Ridley, A. J. (2013) 14-3-3 proteins interact with a hybrid prenyl-phosphorylation motif to inhibit G proteins. *Cell* **153,** 640–653
77. Jaiswal, M., Dvorsky, R., and Ahmadian, M. R. (2013) Deciphering the molecular and functional basis of Dbl family proteins: a novel systematic approach toward classification of selective activation of the Rho family proteins. *J. Biol. Chem.* **288,** 4486–4500
78. Vanhaesebroeck, B., Guillermet-Guibert, J., Graupera, M., and Bilanges, B. (2010) The emerging mechanisms of isoform-specific PI3K signalling. *Nat. Rev. Mol. Cell Biol.* **11,** 329–341
79. Matsunaga-Udagawa, R., Fujita, Y., Yoshiki, S., Terai, K., Kamioka, Y., Kiyokawa, E., Yugi, K., Aoki, K., and Matsuda, M. (2010) The scaffold protein Shoc2/SUR-8 accelerates the interaction of Ras and Raf. *J. Biol. Chem.* **285,** 7818–7826
80. Cordeddu, V., Di Schiavi, E., Pennacchio, L. A., Ma'ayan, A., Sarkozy, A., Fodale, V., Cecchetti, S., Cardinale, A., Martin, J., Schackwitz, W., Lipzen, A., Zampino, G., Mazzanti, L., Digilio, M. C., Martinelli, S., *et al.* (2009) Mutation of SHOC2 promotes aberrant protein N-myristoylation and causes Noonan-like syndrome with loose anagen hair. *Nat. Genet.* **41,** 1022–1026
81. Rodriguez-Viciana, P., Oses-Prieto, J., Burlingame, A., Fried, M., and McCormick, F. (2006) A phosphatase holoenzyme comprised of Shoc2/Sur8 and the catalytic subunit of PP1 functions as an M-Ras effector to modulate Raf activity. *Mol. Cell* **22,** 217–230
82. Ferro, E., and Trabalzini, L. (2010) RalGDS family members couple Ras to Ral signalling and that's not all. *Cell. Signal.* **22,** 1804–1810